

PAPER • OPEN ACCESS

## Aging behavior of ultra-fine grained AA 6061 alloy subjected to constrained groove pressing followed by cold rolling

To cite this article: K Changela *et al* 2019 *IOP Conf. Ser.: Mater. Sci. Eng.* **651** 012069

View the [article online](#) for updates and enhancements.

### Recent citations

- [K. Changela \*et al\*](#)
- [Effect of rolling temperatures on mechanical and fracture behavior of AA 3003 alloy and pure Cu](#)  
Kandarp Changela *et al*



**ECS** **240th ECS Meeting**  
Oct 10-14, 2021, Orlando, Florida

**Register early and save up to 20% on registration costs**

Early registration deadline Sep 13

**REGISTER NOW**

# Aging behavior of ultra-fine grained AA 6061 alloy subjected to constrained groove pressing followed by cold rolling

**K Changela<sup>1,a</sup>, S Kumar<sup>1</sup>, K Hariharan<sup>2</sup> and D Ravi Kumar<sup>1</sup>**

Department of Mechanical Engineering, Indian Institute of Technology Delhi, New Delhi 110016, INDIA

<sup>2</sup> Department of Mechanical Engineering, Indian Institute of Technology Madras, Chennai 600036, INDIA

<sup>a</sup>kandarp.changela06@gmail.com

**Abstract.** A novel severe plastic deformation (SPD) route to achieve strengthening of AA 6061 alloy sheets by subjecting them to constrained groove pressing (CGP) followed by cold rolling (CR) is studied in the present work. Solutionized AA 6061 alloy sheets of 3 mm thickness have been subjected to CGP with an equivalent plastic strain of 1.16. The CGP samples have been subsequently cold rolled to reduce the thickness to 1 mm (67% reduction) to achieve a homogeneous microstructure with ultra-fine grains. It has been observed that yield strength increased significantly due to both CGP and CR. However, the ductility of the processed sample is lower. Therefore, an attempt has been made to study the aging behavior of the processed sample to achieve higher strength along with enhanced ductility through precipitation hardening. Aging of the processed samples was done by isothermal treatment at different temperatures. The microstructure of the deformed and aged samples was characterized by optical microscopy and scanning electron microscopy (SEM). Hardness and tensile tests have been studied to understand the mechanical behavior of deformed and aged samples. From the results, it has been found that processing of this alloy through CGP+CR and subsequent aging improves both strength and ductility due to the combined effect of precipitation hardening and recovery.

## 1. Introduction

Nowadays, research activities are focused on using lightweight materials such as Al and Mg alloys with high strength for application in automobile and other industries in the form of sheets and plates [1, 2]. Heat treatable 6xxx aluminium alloys are widely used in these industries because of their good combination of fatigue strength, corrosion resistance, and formability.

By providing sufficient high strain and proper processing pathways, it is possible to produce high strength materials with nanoscale grain refinement [3]. In 1991, severe plastic deformation (SPD) emerged as a new processing technique to increase the strength of materials by producing ultra-fine grains (UFG) from coarse grain structured materials [4]. In the recent past, several SPD techniques have been developed and studied [5, 6]. However, some of the SPD methods are practically inefficient for sheet or plate-like structure. Cryorolling [7], Accumulative Roll Bonding (ARB), and Constrained Groove Pressing (CGP) are suitable techniques for the processing of metallic sheets. Constrained groove pressing, which was initially proposed



by Shin et al. [8] in 2002, is a promising SPD route to obtain high strength UFG materials. In the CGP process, the specimen is subjected to repetitive shear deformation by deforming alternately between asymmetrically aligned grooved (Figure 1 (a)) and flat dies (Figure 1 (b)) under plane strain condition. Each pass, consisting of four stages, two in the grooved die, and two in a straightening die imposes an effective true strain of 1.16. In this technique, the gap between the upper die and the lower die is equal to the sample thickness, and therefore, the inclined region of the sample, located in the groove, is subjected to pure shear deformation. By imposing more passes, higher strains are imparted to the workpiece. More details about this process could be found in the literature [9].

Based on the previous study of the CGP process, it is concluded that CGP is a suitable route to produce UFG materials without changing the dimensions of the sample using simple dies. The CGP process is versatile and can be used for microstructural refinement for a wide range of metallic materials. However, it is difficult to characterize the CGP samples due to its uneven surface. CGP process is known to impart non-uniform deformation, and hence inherent geometric and microstructural inhomogeneity in the samples is one of the serious issues, which limit its practical application [10]. To overcome these difficulties, the specimen of CGP was subjected to cold rolling. Also, a more recent work [11] showed that further grain refinement is achieved after the rolling of severely deformed samples. The cold rolling followed by SPD alters the microstructure and result in improved strength. However, the room temperature ductility is affected by the subsequent cold rolling [12]. Therefore it is necessary to heat-treat the samples to obtain desired mechanical properties.

In the present work, solutionized AA 6061 alloy sheets have been subjected to CGP. The CGP samples have been subsequently cold-rolled (CR) to reduce the thickness to 1mm (67% reduction). Aging of CGP+CR samples has been done at different temperatures and time to achieve higher strength along with enhanced ductility through precipitation hardening. The mechanical properties and microstructure of deformed and aged samples have been investigated.

## 2. Experimental Procedure

AA 6061 alloy sheets in 'T6' temper condition with a thickness of 3 mm were used as the starting material in the present study. The chemical composition (wt.%) of 0.9% Mg, 0.67% Si, 0.11% Mn, 0.095% Cr, 0.21% Cu, 0.24% Fe, 0.01% Ti, 0.012% Zn and balance Al were used. The samples were cut with dimensions of 108 mm x 108 mm and solution treated at 530°C for two h in a muffle furnace followed by water quenching (as per ASTM B918M). Solutionized (SL) samples were subjected to constrained groove pressing (CGP). Constrained groove pressing experiments were carried out on 300-ton single action hydraulic press at room temperature with an applied load of 60-70 tons. The CGP dies used in the present study are shown in Figure 1. The width and height of the corrugating indents of the grooved die are equal to the sheet thickness. The groove angle and corner radius are 45° and 0.8 mm, respectively. One pass is applied during the CGP process, and it consists of four stages with two corrugated dies, and two straightening dies. The samples processed by CGP were cold rolled with a rolling direction parallel to the grooves, and the thickness reduced to 1mm (67% reduction) with a true strain of 1.09. CGP+CR samples were subjected to artificial aging at 100°C, 130°C, and 190°C for different time (6h to 54h) to understand the age hardening behavior.

The samples for optical microscopy were polished by the standard metallographic procedure to study the microstructural evolution. The samples were etched electrochemically at -15°C and 15 V DC using methanol:perchloric acid (80:20) as the electrolyte. Scanning electron microscopy (SEM) was used to study the precipitates phenomena in aged samples. In order to see the different precipitates after aging, the electropolished samples were etched using 0.5% HF (concentrated) for 30 secs and observed the sample in bright field microscopy.

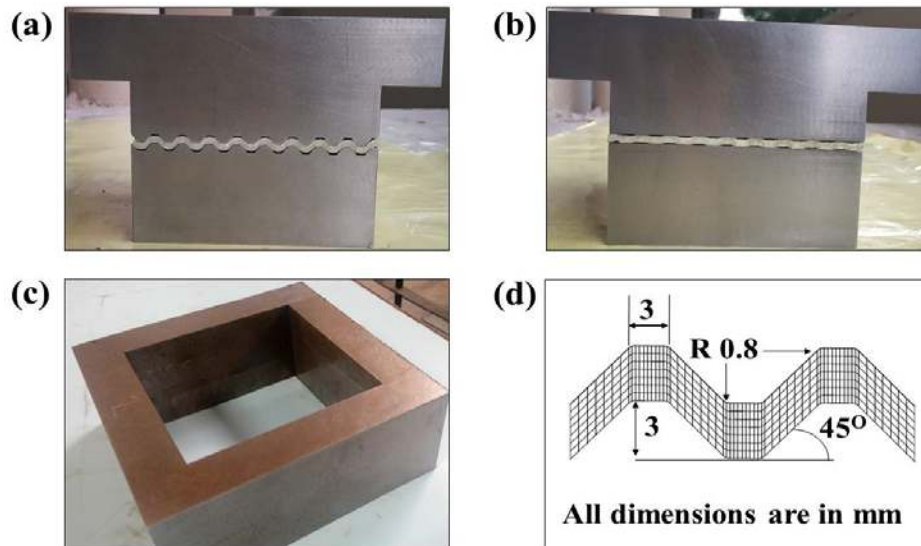


**Figure 1.** CGP dies used in the present study (a) grooving dies, (b) flattening dies, (c) constraining block, and (d) groove geometry.

Tensile and hardness tests were carried out to understand the mechanical properties of deformed and aged samples. In the present work, as deformed samples and aged samples were tested immediately to prevent the influence of natural aging. The tensile samples were cut along the rolling direction of CGP + CR samples and parallel to groove direction of the CGP samples as per ASTM standard E8M. Tensile tests were conducted at room temperature on an INSTRON machine at a constant crosshead speed of 1.92 mm/min with an initial strain rate of  $10^{-3} \text{ S}^{-1}$ . The hardness of all the samples in deformed and aged conditions was measured using a Vickers hardness tester by applying a load of 10 kg for 10 seconds. Hardness was measured parallel to rolling direction in CGP + CR samples, and an average of 10 measurements was taken while in CGP samples, the hardness was measured on the transverse section (perpendicular to groove direction) of the sample. The locations to measure the hardness were chosen with a gap of 5 mm.

### 3. Results and Discussion

#### 3.1 Hardness

The variation of hardness in the solutionized (SL) and CGP samples with the distance in the transverse region (perpendicular to groove direction) are shown in Figure 2. The average hardness of the CGP sample after four stages (effective true strain  $\epsilon = 1.16$ ) is 92 HV, which is 100 % higher than that in the SL condition. A similar hardening behavior of pure Al CGP sample for one pass has been reported earlier [13]. It is seen in Figure 2 that the hardness across the sample width is approximately uniform in the annealed condition and non-uniform in the CGP sample. The non-uniform hardness distribution can be correlated with the inhomogeneity in the grain refinement during CGP. According to Yadav et al. [10] cause of inhomogeneity in the CGP sample is the additional bending strain at the intersection of the two grooves. In addition to the microstructural inhomogeneity, the CGP process imparts geometric inhomogeneity due to the waviness from grooved dies. This geometric inhomogeneity can be overcome by cold rolling the CGP processed sample. It is also possible to obtain additional grain refinement due to cold rolling strain with improved mechanical properties. The evidence of grain refinement has been obtained from hardness results (122 HV), as shown in Figure 3. Figure 4 shows the variation of hardness after isothermal aging treatment of CGP+CR

samples. Four aging temperatures were selected for CGP+CR samples, 100°C, 130°C, 160°C, and 190°C. The aging time was varied in the range of 6-54 h to optimize the aging temperature and time. Recovery and precipitation can simultaneously occur at low-temperature aging resulting in further improvement in strength with higher ductility in heavily deformed materials.

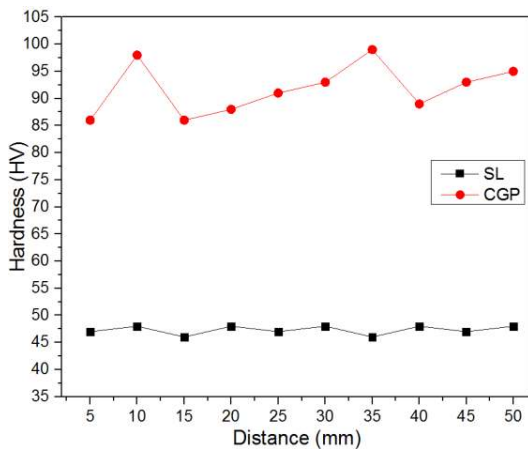


**Figure 2.** Variation of hardness in the transverse section of AA6061 alloy in SL and CGP conditions.

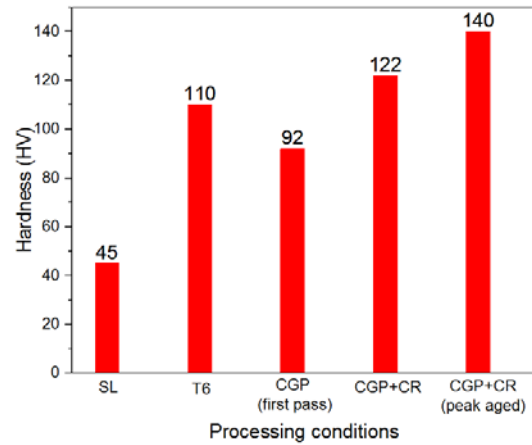


**Figure 3.** Average hardness (in different processed conditions) of AA 6061 alloy.

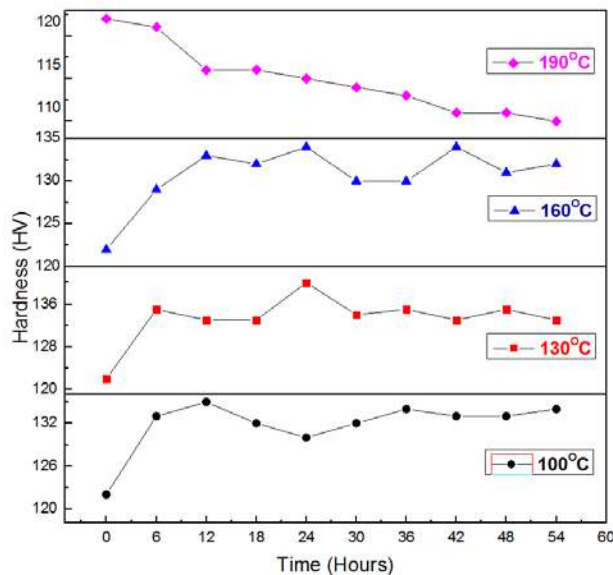


**Figure 4:** Hardness variation in AA 6061 alloy at different temperatures after CGP+CR.

It is shown in Figure 4 that, the hardness increased in sinusoidal variation at all aging temperatures except at 190°C. The hardness gradually decreased at 190°C with aging time due to the effect of recovery, and sub-grain coarsening might have more pronounced than the effect of precipitation hardening at higher temperature. It is reported in the literature [14] that the effect of recovery is well pronounced than the effect of precipitation strengthening during aging of heavily deformed samples at higher temperatures. It is shown in Figure 4 that the hardness increases with aging time for other three aging temperatures (100°C, 130°C, and 160°C), which show that the effect of precipitation hardening is more than the high temperature. It is also observed that, because of the precipitation coarsening (overaging), the hardness decreases after getting the peak hardness value in all three temperatures. An optimum hardness has been observed after aging at 130°C for 24h results in peak-age (PA) condition in CGP+CR sample. An increase in the hardness is about 14% for the peak-aged condition as compared to the CGP+CR condition.

### 3.2 Microstructure

The optical micrographs of solutionized and deformed samples are shown in Figure 5. The microstructure of the solutionized sample shows equiaxed grains with an approximate average size of 88  $\mu\text{m}$  (Figure 5(a)).

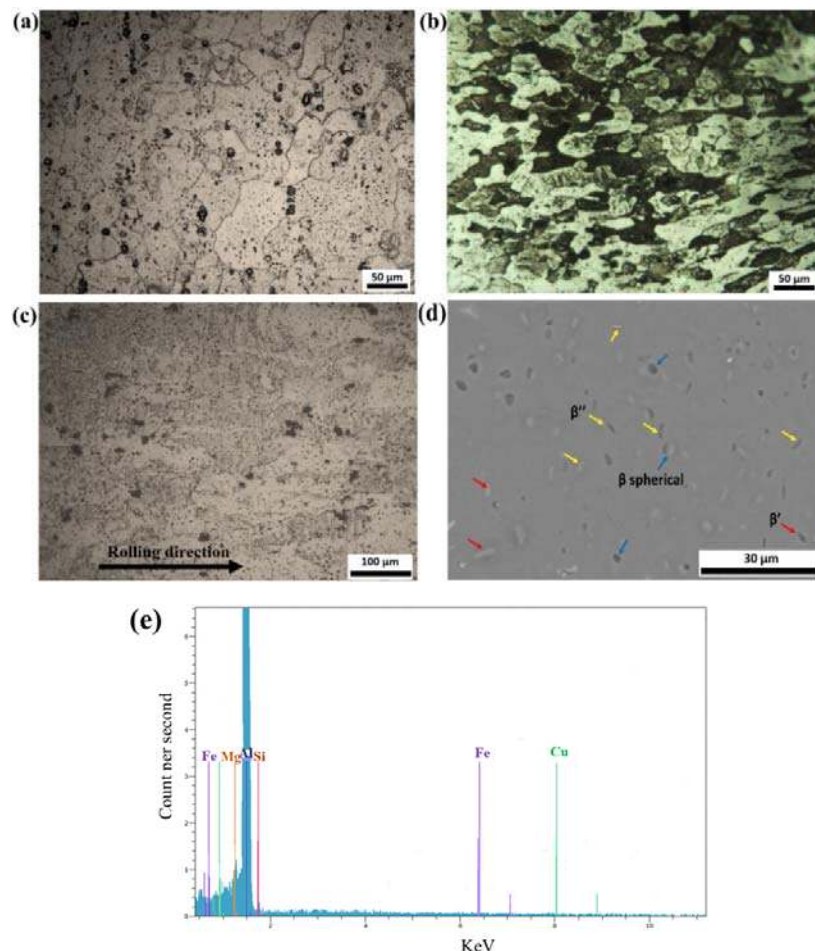


**Figure 5.** Optical micrographs of AA6061 alloy (a) solutionized, (b) CGP (first pass), and (c) CGP+CR; (d) SEM image of CGP+CR (PA) showing precipitates; (e) EDX pattern in CGP+CR (peak aged) condition.

Figure 5 (b) shows the microstructure of the CGP sample after the first pass. Grain refinement in the CGP sample was observed with an approximate average grain size of 18  $\mu\text{m}$ . Cold rolling after CGP gives a more laminate microstructure with elongated grains along the rolling direction (arrow indicates rolling direction), as shown in Figure 5(c). The grains could not be distinguished using an optical microscope due to the severely deformed structure in the material. The microstructure revealed diffused and ill-defined grain boundaries due to severe work hardening at room temperature resulting in fragmentation of grains. AA 6061 alloy sample in CGP+CR (PA) condition was analyzed by using SEM to study the precipitation morphology. Figure 5 (d) shows the SEM image for the PA condition of CGP+CR sample. The microstructure portrays the uniform distribution of precipitates formed after aging of CGP+CR sample at 130°C for 24 h. The precipitation sequence in AA 6061 alloy during aging can be found in the literature [15]. Three types of precipitates, needle-shaped, rod-shaped and spherical shaped have been revealed after aging. Figure 5 (d) shows  $\beta''$  precipitates (indicated by yellow color arrow) with sharp needle shape in the range of 300-400 nm size, rod shape  $\beta'$  precipitates (indicated by red color arrow) in the range of 600-700 nm and large spherical  $\beta$  precipitates, indicated by blue color arrow in the range of 1-2  $\mu\text{m}$ . The evolution of these precipitates corresponding to Fe-rich, Mg-rich, Cu-rich, and Si-rich metastable AlFeCuSi phase and stable  $\text{Mg}_2\text{Si}$  phase is confirmed by EDX analysis as shown in Figure 5 (e). It is reported that a high volume fraction of coherent  $\beta''$  and semi-coherent  $\beta'$  precipitates contribute to the maximum strengthening in Al-Mg-Si alloy compared to incoherent  $\beta$  precipitates [16]. These needle shapes and rod-shaped nanometer-sized precipitates act as obstacles for dislocation movement during the tensile deformation resulting in the strengthening of the sample by dislocation shearing mechanism. In addition to that, with an increase in precipitates density, dislocation density reduced by the annihilation of dislocations. Many researchers observed the presence of dislocation free grains after the aging of SPD material [17].

### 3.3 Tensile Properties

The tensile stress-strain curves for different processing conditions of AA 6061 alloy are shown in Figure 6, and the mechanical properties are summarized in Table 1. The yield strength and ultimate tensile strength of CGP samples are higher (182MPa and 262MPa, respectively) compared to the SL condition in which the values are 100MPa and 174MPa, respectively. The significant increase in tensile strength after CGP (first pass) is mainly due to pure shear deformation during the process leading to work hardening and grain refinement. However, the total elongation of the CGP sample decreased by 72% of the initial condition. The ductility and work hardening exponent ( $n$ ) are less due to lower work hardening rate and inability to accumulate dislocations during subsequent plastic deformation. Further improvement in the strength is observed after the rolling of the CGP sample. The yield strength and ultimate tensile strength of CGP+CR samples are even higher than in T6 condition. However, the ductility sharply decreased from the initial condition, which shows negligible strain hardening ability in CGP+CR samples. It is also observed from Figure 6 and Table 1 that the total elongation of CGP+CR sample is slightly higher than the CGP sample, and this is mainly due to the flat and smooth surface achieved after cold rolling of the CGP sample. The tensile test samples have been cut in the longitudinal direction (parallel to groove direction) of the CGP sample. According to Kumar et al. [9] geometric die features introduce inhomogeneity in the CGP sample, which significantly affects the mechanical properties and hence due to geometric inhomogeneity in the sample, the total elongation is lower for CGP sample.

The peak age (PA) condition (130°C for 24h) of the CGP+CR sample shows the simultaneous improvement in strength and ductility when compared to the CGP+CR sample. The YS and UTS of PA sample are approximately 60% and 21% higher than the T6 condition. In addition to the strength, the ductility of PA condition also increased by 48% from CGP+CR sample. The simultaneous improvement in strength and ductility after aging of CGP+CR sample is attributed to (1) dislocation density decreased due to recovery effect facilitates the more number of dislocations accumulate in the grains and (2) Formation of nanosized precipitates during aging contributes to the improvement in strength. The combined effect of

precipitation hardening and recovery (dislocation annihilation) leads to overall improvement in mechanical properties of PA sample. Panigrahi et al. [18] studied the mechanical properties and microstructure of AA 6063 alloy sample in the cryorolled and aged conditions. They observed that strength improved due to the presence of  $\beta''$  nanosized precipitates and simultaneously ductility improved due to the presence of dislocation free grains after aging.

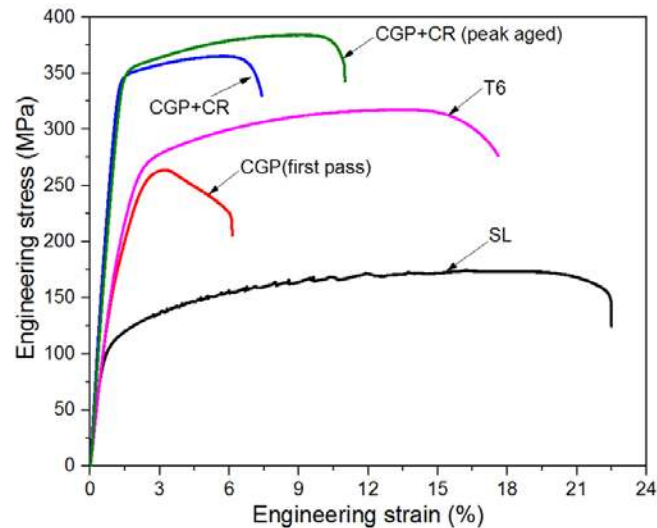


**Figure 6.** Engineering stress-strain curves of AA 6061 alloy.

**Table 1.** Mechanical properties obtained from stress-strain curves of AA 6061 alloy.

Condition	YS (MPa)	UTS (MPa)	Total Elongation (%)	Work Hardening exponent, n
SL	100	174	22.50	0.22
T6	218	317	17.70	0.18
CGP	182	262	6.13	0.19
CGP+CR	341	365	7.43	0.07
CGP+CR (peak aged)	349	386	11.00	0.10

#### 4. Conclusions

The effect of severe plastic deformation (SPD) on microstructure and mechanical properties processed through constrained groove pressing (CGP) of AA6061 was investigated in the present work. The strength of solutionized samples increased by 82 % by imposing a large amount of plastic strain in the material in this route. The further enhancement of strength is achieved by cold rolling of the CGP sample with a smooth and flat surface. It is revealed from the microstructure results that severe grain refinement was observed after the CGP and CGP+CR process. However, the ductility of a deformed sample is very low. Simultaneous improvement of strength and ductility could be achieved by the aging of processed samples at the isothermal condition. Improvement in the strength is due to the presence of  $\beta''$  and  $\beta'$  precipitates in the aged sample while the ductility is increased due to recovery or dislocation annihilation in the structure.

## References

- [1] Satish D R, Kumar D R and Merklein M 2017 *J. Strain Anal. Eng.* **52** (4) 258–273
- [2] Feyissa F T and Kumar D R 2019 *J. Mater. Res. Tech.* **8** (1) 411–423
- [3] Liddicoat P V, Liao X Z, Zhao Y, Zhu Y, Murashkin M Y, Lavernia E J, Valiev R Z and Ringer S P 2010 *Nature Commu.* **1** (6) 1–7
- [4] Valiev R Z, Krasiinikov N A and Tsenev N K 1991 *Mater. Sci. Eng. A.* **137** 35–40
- [5] Zhao B Y, Liao X, Cheng S, Ma E and Zhu Y T 2006 *Adv. Mater.* **18** 2280–2283
- [6] Nurislamova G, Sauvage X, Murashkin M, Islamgaliev R and Valiev R 2008 *Philo. Mag. Lett.* **88** (6) 459–66
- [7] Parmar V, Changela K, Srinivas B, Mani Sankar M, Mohanty S, Panigrahi S K, Hariharan K and Kalyanasundaram D 2019 *Mater.* **12** (2) 1–11
- [8] Shin D H, Park J J, Kim Y S and Park K T 2002 *Mater. Sci. Eng. A.* **328** 98–103
- [9] Kumar S, Hariharan K, Kumar D R and Paul S K 2019 *J. Manu. Process.* **38** 49–62
- [10] Yadav P C, Sinhal A, Sahu S, Roy A and Shekhar S 2016 *J. Mater. Eng. Perf.* **25** (7) 2604–2614
- [11] Mamaghani K R and Kazeminezhad M 2014 *J. Mater. Eng. Perf.* **23** (1) 115–124
- [12] Pouraliakbar H and Jandaghi M R 2018 *Mech. Mater.* **122** 145–158
- [13] Morattab S, Ranjbar K and Reihanian M 2011 *Mater. Sci. Eng. A.* **528** (22–23) 6912–6918
- [14] Kim J K, Jeong H G, Hong S I, Kim Y S and Kim W J 2001 *Scri. Mater.* **45** (8) 901–907
- [15] Yu H, Su L, Lu C, Tieu K, Li H, Li J, Godbole A and Kong C 2016 *Mater. Sci. Eng. A.* **674**, 256–261
- [16] Rao P N, Singh D, Brokmeier H G and Jayaganthan R 2015 *Mater. Sci. Eng. A.* **641** 391–401
- [17] Panigrahi S K and Jayaganthan R 2010 *Metall. Mater. Trans. A.* **41** (10) 2675–2690
- [18] Panigrahi S K and Jayaganthan R 2010 *J. Mater. Sci.* **45** (20) 5624–5636